1156 *Macromolecules* **2010**, *43*, 1156–1158
DOI: 10.1021/ma902522v

Macromolecules
NOTE

Annealing-Induced Oriented Crystallization and Its Influence on the Mechanical Responses in the Melt-Spun Monofilament of Poly(L-lactide)

Bing Na,* Nana Tian, Ruihua Lv, Shufen Zou, and Wenfei Xu

Department of Materials Science and Engineering, East China Institute of Technology, Fuzhou 344000, People's Republic of China

Qiang Fu*

Department of Polymer Science & Materials, Sichuan University, State Key Laboratory of Polymer Materials Engineering, Chengdu 610065, People's Republic of China

Received November 15, 2009; Revised Manuscript Received December 2, 2009

1. Introduction

Poly(L-lactide) (PLLA) is the most promising biodegradable polymer because of its good processability, good biocompatibility, and suitable mechanical properties.[1−4] Similar to other polyesters, such as poly(ethylene terephthalate), PLLA has relatively low crystallization rate under quiescent conditions, and usually it is easy to obtain amorphous state even moderately cooled from the melt.[5−7] However, accelerated crystallization of PLLA is actually observed during melt spinning, as a result of molecular extension under external force.[8,9] Though partial crystallization can be realized during melt spinning, on the other hand, rapid solidification can readily give rise to low crystallinity in the as-spun PLLA fiber. It has been demonstrated that annealing of as-spun fiber below melting temperature is effective to enhance the crystallinity because of cold crystallization. Moreover, the presence of oriented structure in the as-spun fiber favors the cold crystallization during annealing, which becomes more significant with increasing spinning velocity.[8]

To our knowledge, the advent of cold crystallization during annealing must involve structural rearrangements in the amorphous matrix of as-spun PLLA fiber, which is poorly understood yet. Conventional techniques such as X-ray scattering/diffraction measurements are difficult to probe the structural changes in the amorphous matrix, and this dilemma can be readily resolved by Fourier transform infrared spectroscopy, on the other hand.[10]

In this study, a micro-FTIR, composed by a FTIR spectrometer and an IR microscope, is adopted to probe the structural changes in both amorphous and crystalline phase during annealing and subsequent stretching of PLLA monofilament. Combining the video-aid tensile tests, furthermore, the effect of annealing on the mechanical responses of PLLA monofilament is clarified to a large extent.

2. Experimental Section

2.1. Material and Sample Preparation. A commercial poly(L-lactide) (PLLA), supplied by Brightchina Industry Corp., China, was used in this study. It had a viscosity-average molecular weight of about 100 kg/mol, a melt flow index of 17 g/10 min, and a melting point of about 153 °C. Monofilament with a diameter of about 60 μm was melt-spun from a capillary rheometer at 190 °C with a constant take-up speed.

*Corresponding authors: Fax 0086-794-8258320, e-mail bingnash@163.com or bna@ecit.edu.cn (B.N.); Fax 0086-28-85405402; e-mail qiangfu@scu.edu.cn (Q.F.).

2.2. Micro-FTIR Studies. *Annealing*. An as-spun monofilament was first firmly fixed on a plate with clips at two ends and then annealed at 110 °C in an oven. While the desired period was reached, the monofilament in company with the plate was transferred to the sample stage of a Thermo Nicolet infrared microscope. Polarized infrared spectra (by rotating a ZnSe polarizer), parallel and perpendicular to the fiber axis, were collected with a resolution of 4 cm^{-1} at room temperature, and a total of 32 scans were added. The above procedure was repeated for the subsequent annealing period of the same monofilament.

Stretching. The structural transitions during stretching of a monofilament by a mini-stretcher were monitored by the above-mentioned infrared microscope at room temperature. During measurements the monofilament was stretched step by step at a rate of 5 mm/min along the fiber axis. The draw ratio λ, defined as $\lambda = l/l_0$ (l and l_0 was the transient and initial length, respectively), was precisely measured by the extension of an inkmark preprinted on the monofilament.

The dichroic ratio R and structural absorbance A of a desired absorption band were deduced using relations

$$R = A_{\parallel}/A_{\perp} \tag{1}$$

$$A = (A_{\parallel} + 2A_{\perp})/3 \tag{2}$$

where $A_{\parallel}$ and $A_{\perp}$ are the parallel and perpendicular absorbance, respectively.

2.3. Video-Aid Tensile Tests. Mechanical tests of a monofilament were performed on an universal testing machine at room temperature with a crosshead speed of 5 mm/min. A CCD camera (1280 pixel × 1024 pixel), equipped with a tunable magnification lens, was adopted to monitor the longitudinal separation of inkmarks preprinted on the surface of the monofilament during stretching. A reliable draw ratio λ could be obtained through this procedure.

2.4. 2D-SAXS Measurements. Two-dimensional small-angle X-ray scattering measurements on a bundle of monofilaments were conducted on Bruker Nanostar small-angle scattering setup. The wavelength of X-ray was 0.154 nm. The SAXS data were subtracted from background scattering.

2.5. X-ray Diffraction (XRD). XRD measurements were conducted on an X-ray diffractometer equipped with a X-ray generator and a goniometer. The monochromated X-ray from Cu Kα radiation was 0.154 nm. Before measurements the monofilaments were cut into small grains for random arrangements.

 Published on Web 12/15/2009

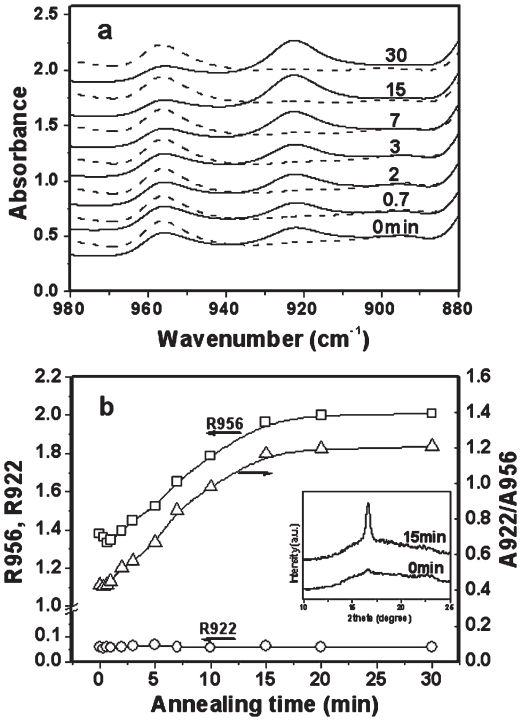

Figure 1. (a) Polarized IR spectra, parallel (dashed lines) and perpendicular (solid lines) to the fiber axis, and (b) the change of R_{956}, R_{922}, and A_{922}/A_{956} during annealing of as-spun PLLA monofilament at 110 °C for a desired period. For comparison, the XRD profiles obtained from the as-spun and annealed (15 min) monofilament is also included in (b) as inset. Note that for clarification vertical shift has been done for all spectra.

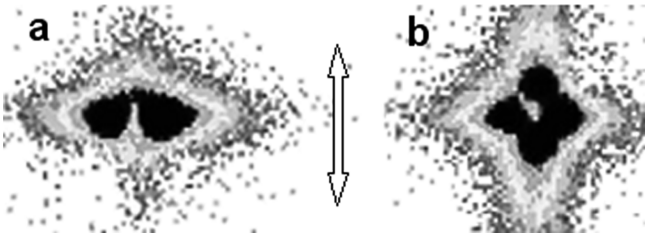

Figure 2. 2D-SAXS patterns obtained from a bundle of (a) as-spun and (b) annealed (15 min) PLLA monofilaments. The arrow indicates the fiber axis.

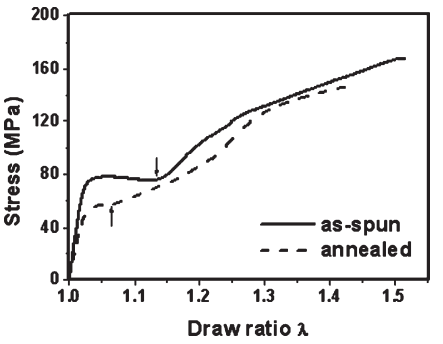

Figure 3. Mechanical responses during stretching of as-spun and annealed (15 min) PLLA monofilament. The arrows in the legend indicate the onset of strain hardening.

3. Results and Discussion

Figure 1 is the structural changes of a PLLA monofilament during annealing as revealed by polarized micro-FTIR measurements. According to pioneering studies,[11,12] the bands at 922 and 956 cm^{-1} are assigned respectively to the crystalline α (or α′) form with a 10_3 helix conformation and to the amorphous phase in the PLLA. Highly oriented fibrillar crystals are indeed formed in the as-spun monofilament, manifested by the nearly absence of absorbance along the fiber axis. Moreover, during annealing the molecular orientation in the crystalline phase keeps almost constant despite that cold crystallization takes place (indicated by increasing ratio of A_{922}/A_{956} and the selective XRD profiles shown in Figure 1b as inset). It means that the initial fibrillar crystals, formed during melt spinning, serve as templates to induce oriented crystallization during annealing. This situation is similar to that encountered in the shear-induced crystallization, where fibrillar structure (shish) can template oriented growth of kebab from the relaxed melt.[13,14] This argument is further evidenced by selective 2D-SAXS patterns shown in Figure 2. The fibrillar crystals in the as-spun monofilament manifest themselves as equatorial streaks. While subjected to annealing at 110 °C for 15 min, additional scattering lobes appear near the beamstop along the meridian, as a result of transverse growth of lamellae induced by the initial fibrillar crystals during cold crystallization. Note that the length of the fibrillar crystals in the as-spun monofilament is relatively short and changes little upon annealing, indicated by the broad meridianal breadth of the equatorial streaks. In such a sense, both as-spun and annealed monofilament can be viewed as discontinuous fiber-reinforced composite where amorphous phase serves as matrix.[15]

On the other hand, cold crystallization during annealing must involve the structural changes in the amorphous matrix. As shown in Figure 1b, the molecular orientation in the amorphous phase (956 cm^{-1} band) first decreases slightly and then increases significantly while cold crystallization sets in. It is expected that, in addition to partial crystallization, the oriented segments in the amorphous phase is frozen due to rapid solidification during melt spinning. While the as-spun monofilament is brought above glass transition temperature (~60 °C), global segmental relaxation can give rise to the decreased molecular orientation in the interfibrillar amorphous regions. Meanwhile, transverse growth of lamellae on the surface of the initial fibrillar crystals during subsequent annealing process could induce local segmental reorientation in the interlamellar amorphous regions,[16] and thus the overall molecular orientation in the amorphous phase is increased again.

Figure 3 is the typical mechanical responses of as-spun and annealed (15 min) monofilament. Common deformation characteristics are observed: under stretching both monofilaments yield first, followed by plastic flow, and finally strain hardening is brought out at large strain. It is indicated that annealing deteriorates the modulus and yield strength and brings the strain hardening in advance, on the other hand. As demonstrated above, both as-spun and annealed monofilaments can be viewed as short fiber-reinforced composites, and little load could be transferred from the amorphous matrix to the oriented crystals at small strain (no more than 0.05).[15] Herein, the mechanical properties should be dominated by the interfibrillar amorphous matrix.[17,18] Decreasing molecular orientation in such interfibrillar regions, in a common sense, could give rise to deteriorated mechanical properties such as modulus and yield strength. With further straining beyond yield point, the plastic event is taken over by the shear deformation of the amorphous matrix. Increasing crystallinity and/or local segmental orientation in the amorphous phase can give rise to earlier onset of strain hardening at large strain. It is the fact observed for the annealed monofilament while the annealing-induced oriented crystallization shown in Figures 1 and 2 is taken into account. Once strain hardening sets in, furthermore, the stress borne by the molecular chains in the

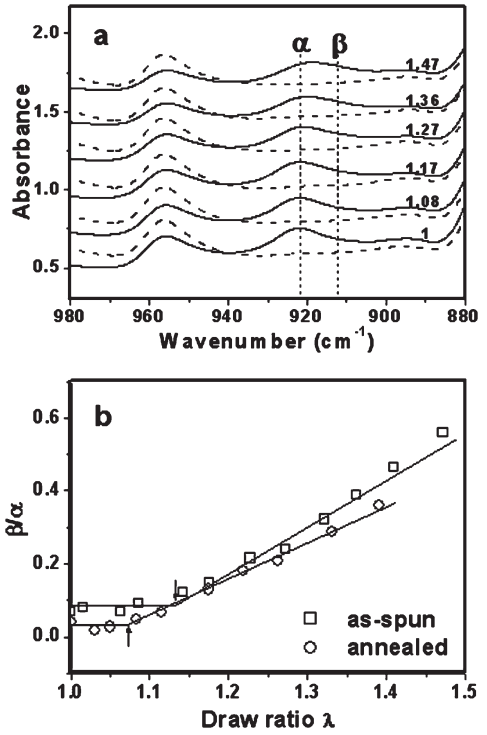

Figure 4. (a) Polarized IR spectra, parallel (dash lines) and perpendicular (solid lines) to the fiber axis, of as-spun PLLA monofilament stretched to indicated draw ratio (numbers in the legend) and (b) draw ratio dependent $\alpha \rightarrow \beta$ crystal transformation during stretching of as-spun and annealed (15 min) monofilament, respectively. Note that for clarification vertical shift has been done for all spectra.

amorphous phase will be transferred to the crystalline phase gradually. As demonstrated by other researchers,[19,20] under stress the initial α-crystals with a 10_3 helical conformation can be converted into β-form with 3_1 helical conformations. In this context, it is expected that there could have some connections between macroscopic strain hardening and microscopic $\alpha \rightarrow \beta$ crystal transformation. As shown in Figure 4, during stretching the initial α-crystals, represented by the 922 cm^{-1} band, are indeed gradually transformed into β-form with a characteristic absorption band at 912 cm^{-1}. The draw ratio corresponding to the sudden transition of β/α (A_{912}/A_{922}) is exactly consistent with that related to the onset of strain hardening in the as-spun and annealed monofilament, respectively. Moreover, more significant strain hardening corresponds to steeper $\alpha \rightarrow \beta$ crystal transformation as a result of higher stress increment during stretching.[20]

4. Conclusion

Transverse growth of lamellae, induced by the initial fibrillar crystals, is indeed observed during annealing of as-spun PLLA monofilament. In company with oriented crystallization, significant structural changes in the amorphous phase occur simultaneously. Upon annealing the segmental orientation in the interfibrillar amorphous regions is relaxed to some extent, whereas the advent of oriented crystallization later gives rise to increased local segmental orientation in the interlamellar amorphous regions. The structural changes in the amorphous matrix are in turn responsible for the deteriorated modulus and yield strength and earlier onset of strain hardening at large strain.

Acknowledgment. This work is supported by the National Natural Science Foundation of China (No. 20704006 and 50973017) and the Project of Jiangxi Provincial Department of Education (No. GJJ08295).

References and Notes

(1) Ikada, Y.; Tsuji, H. *Macromol. Rapid Commun.* **2000**, *21*, 117–132.
(2) Lim, L.; Auras, R.; Rubino, M. *Prog. Polym. Sci.* **2008**, *33*, 820–852.
(3) Jiang, L.; Wolcott, M.; Zhang, J. *Biomacromolecules* **2006**, *7*, 199–207.
(4) Thomson, R.; Wake, M.; Yaszemski, M.; Mikos, A. *Adv. Polym. Sci.* **1995**, *122*, 245–274.
(5) Snchez, M.; Mathot, V.; Poel, G.; Ribelles, J. *Macromolecules* **2007**, *40*, 7989–7997.
(6) Arnoult, M.; Dargent, E.; Mano, J. *Polymer* **2007**, *48*, 1012–1019.
(7) Masirek, R.; Piorkowsk, E.; Galeski, A.; Much, M. *J. Appl. Polym. Sci.* **2007**, *105*, 282–290.
(8) Gupta, B.; Revagade, N.; Hilborn, J. *Prog. Polym. Sci.* **2007**, *32*, 455–482.
(9) Zhou, H.; Green, T.; Joo, Y. *Polymer* **2006**, *47*, 7497–7505.
(10) Meaurio, E.; Lpez-Rodrguez, N.; Sarasua, J. *Macromolecules* **2006**, *39*, 9291–9301.
(11) Zhang, J.; Tsuji, H.; Noda, I.; Ozaki, Y. *J. Phys. Chem. B* **2004**, *108*, 11514–11520.
(12) Pan, P.; Liang, Z.; Zhu, B.; Dong, T.; Inoue, Y. *Macromolecules* **2008**, *41*, 8011–8019.
(13) Yang, L.; Somani, R.; Sics, I.; Hsiao, B.; Kolb, R.; Fruitwala, H.; Ong, C. *Macromolecules* **2004**, *37*, 4845–4859.
(14) Somani, R.; Yang, L.; Hsiao, B.; Sun, T.; Pogodina, N.; Lustiger, A. *Macromolecules* **2005**, *38*, 1244–1255.
(15) Samon, J.; Schultz, J.; Hsiao, B. *Macromolecules* **2001**, *34*, 2008–2011.
(16) Duchesne, C.; Kong, X.; Brisson, J.; Pézolet, M.; Prud'homme, R. *Macromolecules* **2002**, *35*, 8768–8773.
(17) Hu, W.; Buzin, A.; Lin, J.; Wunderlich, B. *J. Polym. Sci., Polym. Phys.* **2003**, *41*, 403–417.
(18) Shioya, M.; Kawazoe, T.; Okazaki, R.; Suei, T.; Sakurai, S.; Yamamoto, K.; Kikutani, T. *Macromolecules* **2008**, *41*, 4758–4765.
(19) Sawai, D.; Takahashi, K.; Sasashige, A.; Kanamoto, T.; Hyon, S. *Macromolecules* **2003**, *36*, 3601–3605.
(20) Takahashi, K.; Sawai, D.; Yokoyama, T.; Kanamoto, T.; Hyon, S. *Polymer* **2004**, *45*, 4969–4976.